Products in the T-State of Aspartate Transcarbamylase: Crystal Structure of the Phosphate and *N*-Carbamyl-L-aspartate Ligated Enzyme[†,‡]

Jingwei Huang and William N. Lipscomb*

Department of Chemistry and Chemical Biology, Harvard University, Cambridge, Massachusetts 02138

Received September 25, 2003; Revised Manuscript Received March 15, 2004

ABSTRACT: The structure of aspartate transcarbamylase of *Escherichia coli* ligated to products (phosphate and *N*-carbamyl-L-aspartate) has been determined at 2.37 Å resolution (*R*-factor = 0.23, R_{free} = 0.27). Results might indicate a product release mode, rather than close analogues to the transition state like those found in our earlier studies of other ligands (*N*-phosphonacetyl-L-aspartate, carbamyl phosphate plus malonate, phosphonoacetamide plus malonate, or citrate plus phosphate). Ordered product release, first carbamylaspartate (CLA) and then phosphate, might be facilitated by a 4 Å movement of phosphate from the substrate−analogue position to the product (phosphate) binding position, and by a somewhat similar release movement of the other product (CLA) relative to its analogue (citrate). This movement is consistent with earlier studies of binding of either pyrophosphate or phosphate alone [Honzatko, R. B., and Lipscomb, W. N. (1982) *J. Mol. Biol. 160,* 265−286].

The first committed step of biosynthesis in the pyrimidine pathway for certain prokaryotes is the reaction of carbamyl phosphate with L-aspartate to form *N*-carbamyl-L-aspartate and phosphate (*1*). This reaction, catalyzed by aspartate transcarbamylase (ATCase),[1] is ordered (*2*): carbamyl phosphate binds before aspartate, and carbamyl aspartate leaves before phosphate. In many organisms, for example, *Escherichia coli*, the pathway leads eventually to cytidine 5′-triphosphate (CTP) and uridine 5′-triphosphate (UTP) prior to biosynthesis of DNA and RNA.

Homotropic regulation by L-aspartate (*3*) occurs if adequate carbamyl phosphate is present, and heterotropic regulation occurs upon activation by ATP and upon inhibition by CTP or by CTP plus UTP (*4*). This regulation helps to achieve a balance between pyrimidines and purines during biosynthesis of RNA and DNA.

The holoenzyme (306 kDa) is a dodecamer (*5*), c_6r_6, composed of catalytic trimers c_3 and regulatory dimers r_2. Each catalytic chain has two domains, one for Asp and the other for carbamyl phosphate. Each regulatory chain has an allosteric domain, which has one binding site for ATP, CTP, or UTP, and a structural but noncatalytic zinc domain (ZN).

Crystallographic studies (*6*) show that the T-to-R transition involves large quaternary conformational changes, including an increase in the intertrimer $c_3 \cdots c_3$ distance by 11 Å, a reorientation about the 3-fold axis of one c_3 relative to the other c_3 by 12°, and a reorientation of each r_2 about its pseudo 2-fold axis by 15°. Studies (*7*) of low angle X-ray scattering in solution suggest that these conformational changes are larger.

Starting with the structure (*8*) of the enzyme liganded to *N*-phosphonacetyl-L-aspartate (PALA), a catalytic mechanism was proposed (*9*) in which the leaving phosphate of carbamyl phosphate is protonated by the NH_2 of aspartate, thus promoting the formation of the new NH−C bond of *N*-carbamyl-L-aspartate. Support came from a structural study (*10*) of binding of carbamyl phosphate (a substrate) plus succinate (an analogue of aspartate). The structure (*11*) of substrate analogues phosphonoacetamide (PAM) and malonate provided support. A very recent study of citrate (an analogue of *N*-carbamyl-L-aspartate, Figure 1) plus phosphate in the R-state gives further support that the binding of PALA is close to that expected for a true substrate analogue. In a recent study at 2.1 Å (*12*), the relevance of the PALA-ligated structure to the probable transition state is supported. Even so, the proton transfer may involve the deprotonated Lys84 in its flexible loop; the mutant K84N (*13*) enzyme shows a 1200-fold reduction in activity. Moreover, the release of phosphate may be assisted by Lys84 (*12*).

In the present study of the T-state bound to products *N*-carbamyl-L-aspartate plus phosphate, the mode of binding might illuminate product release, not efficient substrate binding. The release of carbamylaspartate is probably aided by the movement of phosphate from its position indicated by substrate analogues to a nearby position 4 Å away. This position was seen earlier (*14*) when pyrophosphate alone or phosphate alone binds statistically to the enzyme.

MATERIALS AND METHODS

Crystal Growth. The holoenzyme of *E. coli* aspartate transcarbamylase was isolated by the method of Nowlan and

[†] This work was supported by NIH Grant GM06920.

[‡] Structural data: the coordinates have been deposited with Protein Data Bank as 1R0C.

* To whom correspondence should be addressed. Department of Chemistry and Chemical Biology, Harvard University, 12 Oxford Street, Cambridge, MA 02138, USA. Phone: 617-495-4098. Fax: 617-495-3330. E-mail: lipscomb@chemistry.harvard.edu.

[1] Abbreviations: ATCase, aspartate transcarbamylase; PALA, *N*-phosphonacetyl-L-aspartate; CLA, *N*-carbamyl-L-aspartate; ATP, adenosine 5′-triphosphate; CTP, cytidine 5′-triphosphate; UTP, uridine 5′-triphosphate; PAM, phosphonoacetamide; TS, transition state; PDB, Brookhaven Protein Data Bank; 1D09, the R-state structure of aspartate transcarbamylase with PALA bound deposited in the Protein Data Bank determinated to 2.1 Å resolution; 6AT1, the T-state structure of aspartate transcarbamylase deposited in the Protein Data Bank determinated to 2.6 Å resolution; CP, carbamoyl phosphate; AL, allosteric; Cit, citrate; Pi, phosphate; CHESS, Cornell High Energy Synchrotron Source; rms, root-mean-square.

10.1021/bi0302144 CCC: $27.50
Published on Web 05/06/2004

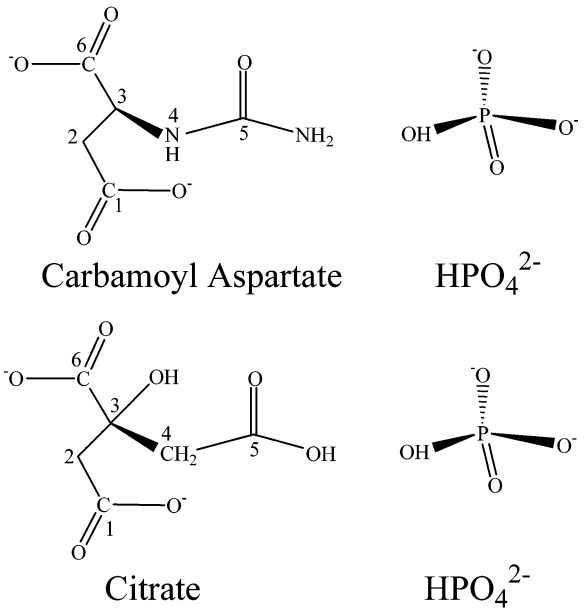

FIGURE 1: The chemical structures of products and their analogues.

Kantrowitz (*15*) from *E. coli* strain EK1104 containing the plasmid pEK54 (*16*). The *N*-carbamyl-L-aspartate (CLA) was synthesized and purified by the method of Zanotti et al. (*17*). The crystals used in this study were grown in the presence of CLA (2 mM) and phosphate (4 mM) by the hanging drop method, where 2 μL of enzyme (16 mg/mL) in buffer (40 mM KH_2PO_4/0.2 mM EDTA/2 mM 2-mercaptoethanol, pH 7.0) was mixed with 2 μL of 12% (vol/vol) poly(ethylene glycol) 4000 (PEG-4K)/0.1 M Hepes-Na (pH 7.5)/3 mM NaN_3, and equilibrated against 1 mL of 12% PEG-4K/0.1 M Hepes-Na (pH 7.5)/3 mM NaN_3.

Data Collection and Analysis. Data were collected at 100° K on beamline F-1 of the Cornell High Energy Synchrotron Source (CHESS). Crystals of the CLA−phosphate−aspartate transcarbamylase complex are in the space group *R*3, and have unit cell dimensions of $a = b = 128.8$ Å, $c = 198.0$ Å, and $\gamma = 120°$. Diffraction data, collected to 2.37 Å, yielded an R_{merge} of 0.064 for 91,954 measured reflections of 46,167 unique reflections. This reduced data set was 95.2% complete in the resolution range 2.37−50 Å. In the asymmetric unit, there are two catalytic and two regulatory chains.

A search model, which contains one catalytic chain and one regulatory chain, was taken from PDB code 1D09 (*12*). Then molecular replacement was carried out by AMORE (*18*). The initial model yielded an initial R factor of 36%, which was reduced to 33% by rigid-body refinement. Models of CLA and phosphate, taken from HIC-UP (*19*), were built into the simulated annealing omit map, and refinement was performed by using the CNS_SOLVE package (*20*). The model was then visualized and modified against $2F_o - F_c$ and $F_o - F_c$ maps using the program O (*21*). Next, the stereochemical properties of the intermediate and the final structures were examined by PROCHECK (*22*). Final refinement yielded $R = 0.226$, $R_{free} = 0.274$, and the Luzzati coordinate error of the final model is 0.37 Å. Protein−protein interface interactions were calculated by Protein−Protein Interaction Server (*23*), and checked by the program O. Figures 2−4 were then prepared using BOBSCRIPT (*24*), MOLSCRIPT (*25*), and PyMOL (*26*).

The planar angle X, which defines the hinge angle between domains (*27*), was calculated by selecting the α-carbon atom coordinates: 5c−32c, 37c−74c, 87c−140c, and 292c−305c for the CP domain; 141c−231c, 248c−269c, and 273c−291c for the Asp domain; 15r−48r and 56r−100r for the AL

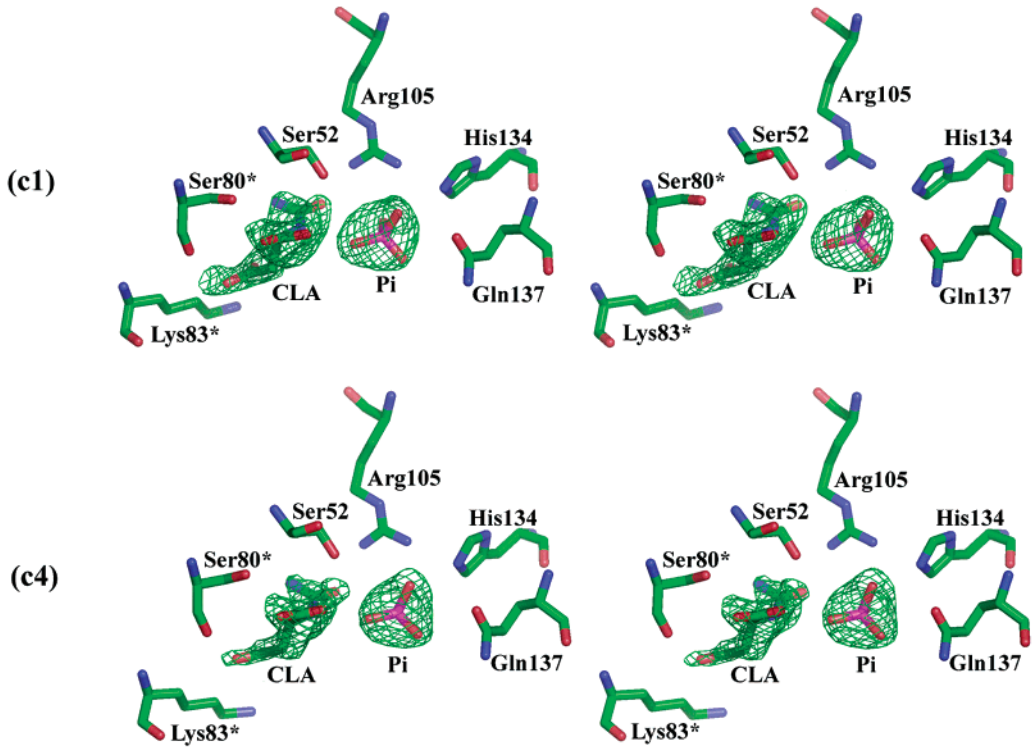

FIGURE 2: A stereo drawing of *N*-carbamyl-L-aspartate (CLA), phosphate (Pi), and some of the active site residues for the two active sites (c1, c4) in one asymmetric unit. The asterisk indicates the residue from an adjacent catalytic chain. The ($F_o - F_c$) omit electron density (3.5σ) around CLA and Pi.

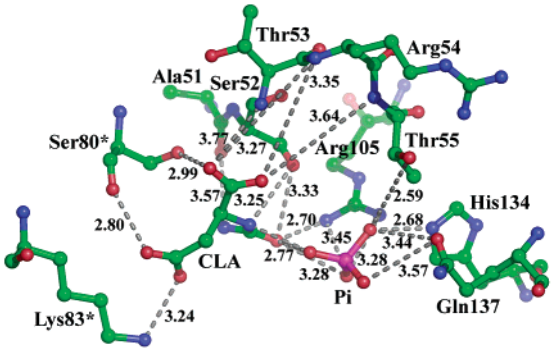

FIGURE 3: *N*-Carbamyl-L-aspartate (CLA) and phosphate (Pi) bound to aspartate transcarbamylase.

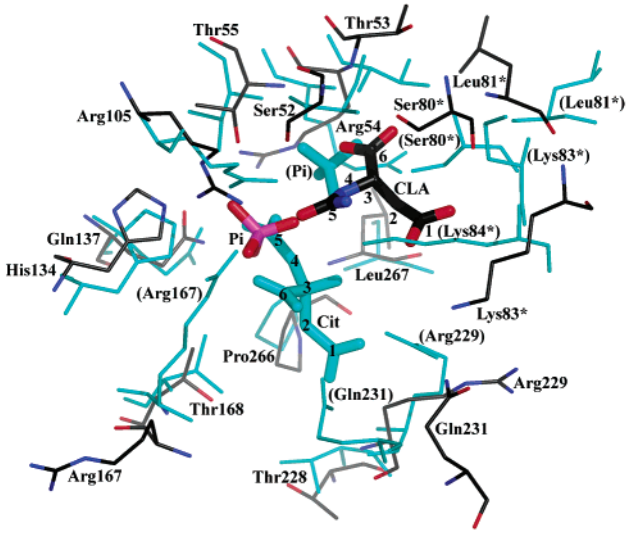

FIGURE 4: The active site superposition of the enzyme complexed with CLA and Pi (Pi is bound to Thr55, Arg105, His134, Gln137, and to CLA in T-form, black-blue-red) and the enzyme complexed with Cit and Pi (Pi is bound to Ser52, Thr53, Arg54, Thr55, Arg105, and Ser80* and Lys84* in R-form, cyan). Some residues of the enzyme complexed with Cit and Pi are indicated in parentheses; the asterisk indicates the residue from an adjacent catalytic chain. Numbers of CLA and Cit are the same as those in Figure 1.

domain; 101r−128r and 134r−149r for the ZN domain. The geometric center of each domain was calculated from the selected α-carbon atom coordinates by MOLEMAN (*28*). The hinges were chosen as follows: the α-carbon atoms of 140c for the Asp and the CP domains, 115r for the CP and ZN domains, and 100r for ZN and AL domains. For the two AL domains from two adjacent regulatory chains, the average coordinate of the two 44r α-carbon atoms was chosen as the hinge. Superposition of the structures and the relative rotation between domains as well as the rms deviation were calculated by LSQMAN (*29*).

RESULTS

The Extended (Extreme) T-State. The noncrystallographic symmetry between the two catalytic chains (rms deviation of 0.15 Å) or the two regulatory chains (rms deviation of 0.21 Å) in the asymmetic unit of the CLA/phosphate complex provides an upper bound for reference. To some extent, it may include distortion due to intermolecular interactions.

In the CLA/phosphate ATCase structure, the $c_3 \cdots c_3$ distance is 45.3 Å, slightly less than the $c_3 \cdots c_3$ distance of 45.5 Å in the unligated T structure, 6AT1 (*30*). In addition, the c_3 to c_3 relative rotation is increased by 2.5°, and the rotation of each regulatory dimer about its pseudo 2-fold axis is increased by 1.2° in the new structure over the value for 6AT1 structure. These changes are comparable with those in the Thr82-to-Ala mutant (PDB code 1NBE) designated as an extreme T-state (*27*).

Further comparison of the CLA/phosphate structure with the unligated T-state shows that the X-planar angles between domains are more open in the new structure by 2.0−3.5° between Asp and CP domains and 1.6° between CP and ZN domains, but more closed by 2.6° between ZN and AL domains and 2.1° between two AL domains. The larger X-planar angles of 2.0−3.5° between Asp and CP domains is of special interest with respect to a probable product leaving mechanism.

The CLA/Phosphate Binding Sites. The two active sites in one asymmetric unit show very similar binding modes (Figure 2). One difference is that one H_2O bound to both CLA and phosphate in chain c1 (top trimer: c1,c2,c3) is not present in chain c4 (bottom trimer: c4,c5,c6). [Regulatory dimers are r1,r6; r2,r4; and r3,r5].

Unexpectedly, the binding of both CLA and phosphate (Figure 3) differs from the binding modes shown by transition state (TS) mimics: (I) PALA (*8*, *12*), (II) carbamyl phosphate plus succinate (*10*), (III) phosphonoacetamide plus malonate (*11*), and (IV) citrate and phosphate (*37*, the preceding paper in this issue). For example, the complex of ATCase with CLA/phosphate is compared with that the enzyme complexed with citrate/phosphate in Figure 4. Thus, the phosphate has moved 4 Å to a new site which is adjacent to that found in TS analogues. These two sites, 4 Å apart, have been previously identified in the complex of ATCase with pyrophosphate (*14*), and also found with partial occupancy in the complex with phosphate (*14*), which is present equally at a 50% level in each of the two sites.

The CLA, on the other hand, shows binding in a new site which is near the now vacant original phosphate site. The new structure shows that no residues block the probable leaving pathway for CLA. Clearly, the process suggested here allows CLA to leave the enzyme before phosphate leaves from its new site.

DISCUSSION

The present study of binding of products (phosphate and CLA) to the T-state places phosphate at a new position 4 Å away from the site (here called the reference position) expected on the basis of binding to the R-state of substrates, analogues and PALA. For example, carbamyl phosphate (a real substrate) and succinate established (*10*) the reference position for its phosphate in the R-state. Also, phosphonoacetamide when bound to the T-form indicates (*11*) this same reference position for its phosphate. Actually, an earlier study (*14*) showed that both positions were occupied when pyrophosphate alone bound to the T-state, and at about one-half occupancy (to avoid crowding) when phosphate alone was bound to the T-state.

The CLA is also bound to the T-state in a way that is unexpected. Its binding does not resemble closely the atomic positions expected for CLA from R-state structure studies of substrate (carbamyl phosphate), analogues and PALA.

Other structural studies of reactions in the T-state may show some limited generality of these new states. Carbamylation of two aspartate analogues, cysteine sulfinate

Table 1: Comparison between the New T Structure and T-State or R-State Structure

	new structure compare to unliganded T-state structure[a]		new structure compare to PALA liganded R-state structure[b]	
	residue region	rms deviation (Å)	residue region	rms deviation (Å)
catalytic chain			c47−c54	1.6−3.4
	c75−c79	1.6−5.8	c74−c97	1.7−4.4
	c81−c83	3.0−3.7	c105−c124	1.6−2.5
	c85−c86	1.5−1.9	c128−c134	1.8−2.2
			c164−c167	1.6−1.8
	c233−c234	1.9	c189−c200	1.5−2.5
	c244−c246	3.0−6.6	c231−c246	3.9−11.5
	c309−c310	2.0−2.1	c308−c310	2.8−5.4
	c1−c310	0.9	c1−c310	2.2
regulatory chain	r10−r13	1.3−3.2	r10−r13	1.7−2.3
	r49−r54	1.4−2.9	r117−r122	1.5−2.9
	r88−r90	1.4−2.4	r130−r131	1.5−2.7
	r129−r132	1.5−7.0	r148−r150	1.5−2.2
	r8−r153	1.3	r1−r153	2.9

[a] PDB code 6AT1 (*30*). [b] PDB code 1D09 (*12*).

Table 2: Polar Interface Interactions in the New Structure[a]

c1−c2	c1−c4	c1−r1	c1−r4	r1−r6
His41−Glu37		Ser11−Glu142		Leu7−Glu10
Ser69−His64		Thr87−Glu119		Glu10−Leu7
Val70−His64		*Leu88−Glu119		Glu10−Glu10
Gly72−Arg56		*Ala89−Glu119		Gln24−Thr36
Asn78−Asn78		Pro107−Asn113		Thr36−Gln24
Thr79−Thr53		Gln108−Asn113		Thr38−Asn47
Ser80−*Ser52		*Glu109−Asn113		Asp39−Asn47
Ser80−*Thr53		Glu109−Asn113		Asp39−Arg55
Ser80−Thr53		Glu109−Asn111		Gln40−Asn47
*Ser80−Thr53		Glu109−*Ile115		Ile42−*Ile46
Lys83−Gln231		*Gly110−Tyr140		Ile42−Leu46
Asp90−Arg269		Arg113−Glu142		*Ile42−Leu46
Thr97−Gly290		Glu117−Lys139		Ile44−Ile44
Tyr98−Arg54		Glu117−Tyr140		Ile44−*Ile44
Tyr98−Arg65	Ser131−Asp236	Ser131−Lys143		*Leu46−Ile42
Asp100−Arg65	Lys164-Glu239	Asn132−Cys141		Leu46−*Ile42
	Tyr165−Glu239	Asn132−Glu142		Leu46−Ile42
	Asp236−Ser131	Gln133−Glu142	Asp236−Ala131	Asn47−Thr38
	Glu239−Lys164		Asp236−Ile134	Asn47−Asp39
	Glu239−Tyr165		Ser238−Asn111	Asn47−Gln40
				Arg55−Asp39

[a] All interactions with distance less than 3.8 Å between nitrogen and oxygen are shown. The polar interactions of c6−r6 interface are similar to that of c1−r1, and the polar interactions of c6−r3 interface are similar to that of c1−r4. Asterisks indicate backbone nitrogen.

$^{+}H_3NCH(CO_2^{-})CH_2SO_2^{-}$ (*31*) or L-alanosine $^{+}H_3NCH(CO_2^{-})$-$CH_2N(OH)NO$ (*32*), show noncooperative kinetics, and other kinetic evidence of T-state behavior. Crystallization should be attempted from enzyme plus one or the other of these aspartate analogues plus carbamyl phosphate or phosphonoacetamide. In another projected study acetyl phosphate in place of carbamyl phosphate (*33*) may be enough different so that the T-state is favored, for this analogous reaction.

Under conditions in which other enzymes remove aspartate rapidly, the reverse reaction occurs in the T-state (*34*). The new positions for phosphate and CLA in this structural study present a starting point for the reverse reaction in the T-state. In one possible sequence of events leading to reaction, the CLA and phosphate might move considerably to reach the positions near the citrate-phosphate of the R-state (Figure 4). Another sequence keeps the reverse reaction entirely in the T-state by employing the new phosphate and CLA positions with comparatively little movement to yield carbamyl phosphate and Asp. Further kinetic studies may reveal the large movement if it occurs, and structural studies of analogues may test whether the new phosphate site is also adopted for carbamyl phosphate or its analogues. Studies of forward and reverse processes in mutants which do not undergo the T-to-R transition may also be informative.

Finally, the new sites for Pi and CLA may represent an intermediate stage between product formation in either the R-state or the T-state and product release in the T-state. Further studies are required to tell whether other "frozen T" states show this stage. Product leaving from the T-state is usually offered as preferred (*35*, *36*), although at higher but nonsaturating substrate concentration release of product is to be expected from the R-state.

ACKNOWLEDGMENT

This work is based upon research conducted at the Cornell High Energy Synchrotron Source (CHESS), which is supported by the National Science Foundation under award DMR 97-13424, using the Macromolecular Diffraction at CHESS (MacCHESS) facility, which is supported by award RR-01646 from the National Institutes of Health, through its National Center for Research Resources.

APPENDIX

Table 1 shows the comparison between the new T structure and T-state or R-state structure, and Table 2 shows the polar interface interactions in the new structure.

REFERENCES

1. Yates, R. A., and Pardee, A. B. (1956) Control of pyrimidine biosynthesis in *E. coli* by a feedback mechanism, *J. Biol. Chem. 221*, 743−756.
2. Wedler, F. C., and Gasser, F. J. (1974) Ordered substrate binding and evidence for a thermally induced change in mechanism for *E. coli* aspartate transcarbamylase, *Arch. Biochem. Biophys. 163*, 57−68.
3. Gerhart, J. C., and Pardee, A. B. (1962) Enzymology of control by feedback inhibition, *J. Biol. Chem. 237*, 891−896.
4. Wild, J. R., Loughrey-Chen, S. J., and Corder, T. S. (1989) In the presence of CTP, UTP becomes an allosteric inhibitor of aspartate transcarbamylase, *Proc. Natl. Acad. U.S.A. 86*, 46−50.
5. (a) Weber, K. (1968) New structural model of *E. coli* aspartate transcarbamylase and the amino acid sequence of the regulatory polypeptide chain, *Nature 218*, 1116−1119. (b) Wiley, D. C., and Lipscomb, W. N. (1968) Crystallographic determination of symmetry of aspartate transcarbamylase: studies of trigonal and tetragonal crystalline forms of aspartate transcarbamylase show that the molecule has a three-fold and a two-fold symmetry axis, *Nature 218*, 1119−1121.
6. Ladner, J. E., Kitchell, J. P., Honzatko, R. B., Ke, H. M., Volz, K. W., Kalb, A. J., Ladner, R. C., and Lipscomb, W. N. (1982) Gross quaternary changes in aspartate carbamoyltransferase are induced by the binding of *N*-(phosphonacetyl)-L-aspartate: a 3.5-Å resolution study, *Proc. Natl. Acad. Sci. U.S.A. 79*, 3125−3128.
7. Svergun, D. I., Barberato, C., Koch, M. H. J., Fetler, L., and Vachette, P. (1997) Large differences are observed between the crystal and solution quaternary structures of allosteric aspartate transcarbamylase in the R-state, *Proteins 27*, 110−117.
8. Ke, H. M., Lipscomb, W. N., Cho, Y., and Honzatko, R. B. (1988) Complex of N-phosphonacetyl-L-aspartate with aspartate carbamoyltransferase: X-ray refinement, analysis of conformational changes and catalytic and allosteric mechanisms, *J. Mol. Biol. 204*, 725−747.
9. Gouaux, J. E., Krause, K. L., and Lipscomb, W. N. (1987) The catalytic mechanism of *Escherichia coli* aspartate carbamoyltransferase: a molecular modeling study, *Biochem. Biophys. Res. Commun. 142*, 893−897.
10. Gouaux, J. E., and Lipscomb, W. N. (1988) Three-dimensional structure of carbamoyl phosphate and succinate bound to aspartate carbamoyltransferase, *Proc. Natl. Acad. U.S.A. 85*, 4205−4208.
11. Gouaux J. E., and Lipscomb W. N. (1990) Crystal structures of phosphonoacetamide ligated T and phosphonacetamide and malonate ligated R states of aspartate carbamoyltransferase at 2.8 Å resolution and neutral pH, *Biochemistry 29*, 389−402.
12. Jin, L., Stec, B., Lipscomb, W. N., and Kantrowitz, E. R. (1999) Insights into the mechanisms of catalysis and heterotropic regulation of *Escherichia coli* aspartate transcarbamylase based upon a structure of the enzyme complexed with the bisubstrate analogue *N*-phosphonacetyl-L-aspartate at 2.1 Å, *Proteins: Struct., Funct., Genet. 37*, 729−742.
13. Robey, E. A., Wente, S. R., Markby, D. W., Flint, A., Yang, Y. R., and Schachman, H. K. (1986) Effect of amino acid substitutions on the catalytic and regulatory properties of aspartate transcarbamylase, *Proc. Natl. Acad. U.S.A. 83*, 5934−5938.
14. Honzatko, R. B., and Lipscomb, W. N. (1982) Interactions of phosphate ligands with *Escherichia coli* aspartate carbamoyltransferase in the crystalline state, *J. Mol. Biol. 160*, 265−286.
15. Nowlan, S. F., and Kantrowitz, E. R. (1985) Superproduction and rapid purification of *E. coli* aspartate transcarbamylase and its catalytic subunit under extreme derepression of the pyrimidine pathway, *J. Biol. Chem. 260*, 14712−14716.
16. Xu, W., Pitts, M. A., Middleton, S. A., Kelleher, K. S., and Kantrowitz, E. R. (1988) Propagation of allosteric changes through the catalytic-regulatory interface of *Escherichia coli* aspartate transcarbamylase, *Biochemistry 27*, 5507−5515.
17. Zanotti, G., Monaco, H. L., and Foote, J. (1984) Structure of the inhibitor of aspartate transcarbamylase *N*-(phosphonacetyl)-L-aspartate, *J. Am. Chem. Soc. 106*, 7900−7904.
18. Navaza, J. (1994) *AMoRe*: an automated package for molecular replacement, *Acta Crystallogr., Sect. A: Found. Crystallogr. 50*, 157−163.
19. Kleywegt, G. J., and Jones, T. A. (1998) Databases in protein crystallography, *Acta Crystallogr., Sect. D: Biol. Crystallogr. 54*, 1119−1131.
20. Brunger, A. T., Adams, P. D., Clore, G. M., DeLano, W. L., Gros, P., Grosse-Kunstleve, R. W., Jiang, J.-S., Kuszewski, J., Nilges, N., Pannu, N. S., Read, R. J., Rice, L. M., Simonson, T., and Warren, G. L. (1998) Crystallography and NMR system (CNS): A new software system for macromolecular structure determination, *Acta Crystallogr., Sect. D: Biol. Crystallogr. 54*, 905−921.
21. Jones, T. A., Zou, J.-Y., Cowan, S. W., and Kjeldgaard, M. (1991) Improved Methods for Building Protein Models in Electron Density Maps and the Location of Errors in these Models, *Acta Crystallogr., Sect. A: Found. Crystallogr. 47*, 110−119.
22. Laskowski R. A., MacArthur M. W., Moss D. S., and Thornton J. M. (1993) PROCHECK: A program to check the stereochemical quality of protein structures, *J. App. Crystallogr. 26*, 283−291.
23. Jones, S., and Thornton, J. M. (1996) Principles of Protein−Protein Interactions Derived From Structural Studies, *Proc. Natl. Acad. U.S.A. 93*, 13−20.
24. Esnouf, R. M. (1999) Further additions to *MolScript* version 1.4, including reading and contouring of electron-density maps, *Acta Crystallogr., Sect. D: Biol. Crystallogr. 55*, 938−940.
25. Kraulis, P. J. (1991) MOLSCRIPT: a program to produce both detailed and schematic plots of protein structures, *J. App. Crystallogr. 24*, 946−950.
26. Delano, W. N. (2002) The PyMOL molecular graphic system, San Carlos, CA, Delano Scientific.
27. Williams, M. K., Stec, B., and Kantrowitz, E. R. (1998) A single mutation in the regulatory chain of *Escherichia coli* aspartate transcarbamylase results in an extreme T-state structure, *J. Mol. Bol. 281*, 121−134.
28. Kleywegt, G. J., and Jones, T. A. (1997) Detecting folding motifs and similarities in protein structures, *Methods Enzymol. 277*, 525−545.
29. Kleywegt, G. J. (1999) Experimental assessment of differences between related protein crystal structures, *Acta Crystallogr., Sect. D: Biol. Crystallogr. 55*, 1878−1884.
30. Stevens, R. C., Gouaux, J. E., and Lipscomb, W. N. (1990) Structural consequences of effector binding to the T state of aspartate carbamoyltransferase: crystal structures of the unligated and ATP- and CTP-complexed enzymes at 2.6 Å resolution, *Biochemistry 29*, 7691−7701.
31. Foote, J., Lauritzen, A. M., and Lipscomb, W. N. (1985) Substrate specificity in aspartate transcarbamylase; interaction of the enzyme with analogs of aspartate and succinate, *J. Biol. Chem. 260*, 9624−9629.
32. Ballion, J., Tauc, P., and Hervé, G. (1985) A noncooperative substrate for *Escherichia coli* aspartate transcarabamylase, *Biochemistry 24*, 7182−7187.
33. Hervé, G. (1989) In *Allosteric Enzymes*, Chapter 12, CRC Press, Boca Raton, FL.
34. Foote, J., and Lipscomb, W. N. (1981) Kinetics of aspartate transcarbamylase from *Escherichia coli* for the reverse direction of reaction, *J. Biol. Chem. 256*, 11428−11433.
35. Hsuanyu, Y., and Wedler, F. C. (1988) Effectors of *Escherichia coli* aspartate transcarbamoylase differentially perturb aspartate binding rather than the T−R transition, *J. Biol. Chem. 263*, 4172−4181.
36. Lee, B. H., Ley, B. W., Kantrowitz, E. R., O'Leary, M. H., and Wedler, F. C. (1995) Domain closure in the catalytic chains of *Escherichia coli* asparate transcarbamoylase influence the kinetic mechanism, *J. Biol. Chem. 270*, 15620−15627.
37. Huang, J., and Lipscomb, W. N. (2004) Aspartate Transcarbamylase (ATCase) of *Escherichia coli*: A New Crystalline R-State Bound to PALA, or to Product Analogues Citrate and Phosphate, *Biochemistry 43*, 6415−6421.

BI0302144